16 Physics of Biological Systems

Conrad Escher, Hans-Werner Fink, Patrick Helfenstein (until 12.2012), Alina Horwege (until 10.2012), Tatiana Latychevskaia, Jean-Nicolas Longchamp, Mirna Saliba, Jonas Verges (since 01.2013), and Flavio Wicki

In collaboration with: Prof. Philippe Dumas, CNRS Strasbourg (France); Eugen Ermantraut, Clondiag Chip Technologies GmbH (Germany); Prof. Bruno Klaholz, University of Strassbourg (France); Prof. Jannik C. Meyer, University of Vienna (Austria); Prof. Ute Kaiser, University of Ulm (Germany); Dr. Ilona Müllerová and Dr. Luděk Frank, Institute of Scientific Instruments, Brno (Czech Republic); Dr. Soichiro Tsujino, PSI (Switzerland); Dr. Fabio Lamattina and Dr. Ivan Shorubalko, EMPA Dübendorf (Switzerland)

The structural investigation of individual biological objects by employing coherent low-energy electrons is the primary goal of our research. It involves in-line holography with low energy electrons, Fourier transform holography as well as coherent diffraction imaging and is assisted by micro-structuring techniques using a focused gallium ion beam as well as a focused helium ion beam available to us at the Swiss Federal Laboratories for materials science and technology (EMPA) in Dübendorf. Our current activities are divided in the following interconnected individual projects:

- Electron Holography and Coherent Diffraction
  Major experimental challenges are to improve the interference resolution, establish methods for creating free standing thin carrier films of graphene transparent for low-energy electrons as well as appropriate techniques to present a single protein to the coherent electron wave front. Next to these technical issues, a second, equally important requirement for achieving high resolution structural information is the reconstruction of the electron holograms; i.e., the iterative phase retrieval in coherent diffraction. This is achieved by developing numerical algorithms for the integrals governing these coherent optics problems.

- Fourier Transform Holography (FTH)
  FTH with low-energy electrons is a high resolution lens-less imaging method based on the use of an extended reference where a specimen of biological or non-biological nature is non-destructively imaged. The recording is performed by illuminating the specimen and reference object or pinhole with a parallel beam of low-energy electrons. The interference between the wave scattered by the specimen and the reference wave results in a holographic diffraction pattern. Its Fourier transform represents the autocorrelation of the transmission function of the specimen under study.

- Electron and Ion Point Sources
  Field Ion Microscopy and related techniques are employed when fabricating or operating novel electron and ion point sources. In collaboration with PSI, field emitter arrays are characterised and specified for their use as bright electron sources for the X-Ray Free Electron Laser (XFEL) project.

- DNA and Proteins in liquids
  The aim is to directly observe the dynamics of single DNA molecules in liquids by video fluorescent microscopy. In combination with molecular anchoring techniques, adopted from Clondiag Chip Technologies in Jena, we also address the energetics of the molecule. We designed DNA modifications for attaching fluorescent proteins which shall help us to obtain structural information about proteins in vacuum using electron holography and coherent diffraction. Thermal desorption spectroscopy of water from fluorescent proteins shall help us to judge under what thermal conditions proteins remain in their native state in a vacuum environment.

Selected recent achievements referring to the past year shall be discussed in some more detail below.

16.1 Coherent Diffraction Imaging (CDI)

Most of the protein structural information available today has been obtained from crystallography experiments by means of averaging over many molecules assembled into a crystal. Since biological molecules exhibit different conformations, averaging smears out structural details. That is why a strong desire to gain structural data from just a single molecule is emerging. Electrons with kinetic energies below 200 eV are the only radiation known today where elastic scattering dominates. Radiation damage-free imaging of a single biological molecule is thus possible by recording holograms and coherent low-energy electron diffraction patterns [1].

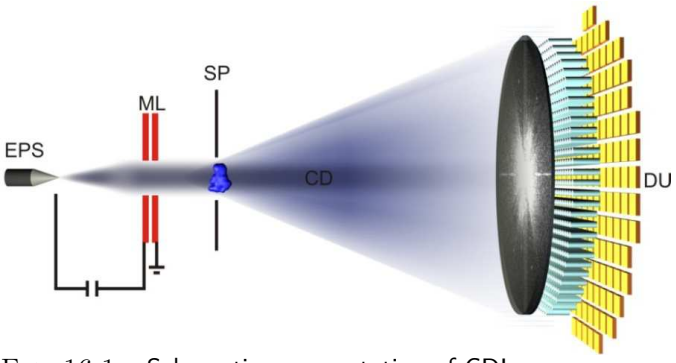

FIG. 16.1 – Schematic representation of CDI.
EPS: coherent electron point source
ML: low-aberration micro-lens to form a parallel electron wavefront
SP: sample embedded inside the coherent electron beam
CD: coherent diffraction pattern
DU: electron detector unit with high spatial resolution and fulfilling the oversampling condition.

FIG. 16.2 – Dedicated sample holder to guarantee almost zero-field conditions between sample and detector. The opening angle of the cone provides a qualitative impression of the very large aperture of this microscope.

16.1.1 Recent experimental achievements

We have embarked upon using the damage-free radiation provided by coherent low-energy electrons to realise CDI and have recently been able to achieve a resolution of 2Å in imaging a freestanding graphene sample. The overall CDI setup is sketched in Fig. 16.1. A sharp tungsten tip acts as an electron point source emitting a coherent spherical wave with kinetic energies between 50 and 300 eV. A micro-lens placed a few microns away from the electron emitter forms a coherent parallel wave that impinges onto a sample some distance behind the lens. At a distant detector, the intensity of the diffraction pattern corresponding to the square amplitude of the Fourier transform of the object is recorded with high spatial resolution. In order to sample this pattern with sufficiently high frequency to match the oversampling requirement, the object must be surrounded by a no-density region.

Our ultra-high vacuum diffraction microscope has been designed and built featuring a dedicated detector system of 75 mm in diameter exhibiting a spatial resolution of about 20 μm. On the ambient pressure side, the fibre optic plate is coupled to a high-resolution CCD chip (Sinar AG, Zurich) with 8000×6000 pixels and a dynamics of 16 bit. As expected, the down-scaling of the electrostatic lens with a 1 micrometer-diameter bore leads to down-scaled spherical aberrations comparable to high end commercial microscopes [2]. By means of this lens, a parallel coherent low-energy wavefront is formed that impinges onto the sample. Since there is no further lens beyond the sample, the numerical aperture of he system can be made wide open without being concerned with growing lens aberrations. In conventional high-resolution TEM, beam-limiting apertures need to be introduced such that the deviation from the optical axes is limited to a few mrad while in our setup 0.5 rad can be easily achieved. In fact, in our setup there is no beam-limiting aperture present but the opening angle is rather given by the detector diameter and the distance from the sample. However, special care needs to be exercised to guarantee an absolute field-free region between sample and detector. First experiments showed slightly asymmetric diffraction patterns and initially we suspected magnetic fields to be the cause. A series of control experiments revealed that rather electrostatic stray-fields were resposible for the effect which has now been eliminated by the dedicated sample holder shown in Fig. 16.2. The piece is made from titanium, gold plated, and mounted on a four-axis manipulator enabling accurate centring of the sample in the electron beam.

16.2 Merging Holography and CDI into HCDI

Recently, we revealed the relationship between the hologram and the diffraction pattern of an object, which allows holography and coherent diffraction imaging (CDI) to be combined into a superior technique: holographic coherent diffraction imaging (HCDI). HCDI inherits fast and reliable reconstruction from holography and the highest possible resolution from CDI [3].

16.2.1 The HCDI algorithm

The Fourier transform of an in-line hologram is proportional to the complex-valued object wave in the far-field. This relationship is illustrated for experimental images in Fig. 16.3. The phase distribution of the Fourier transform of the in-line hologram provides the

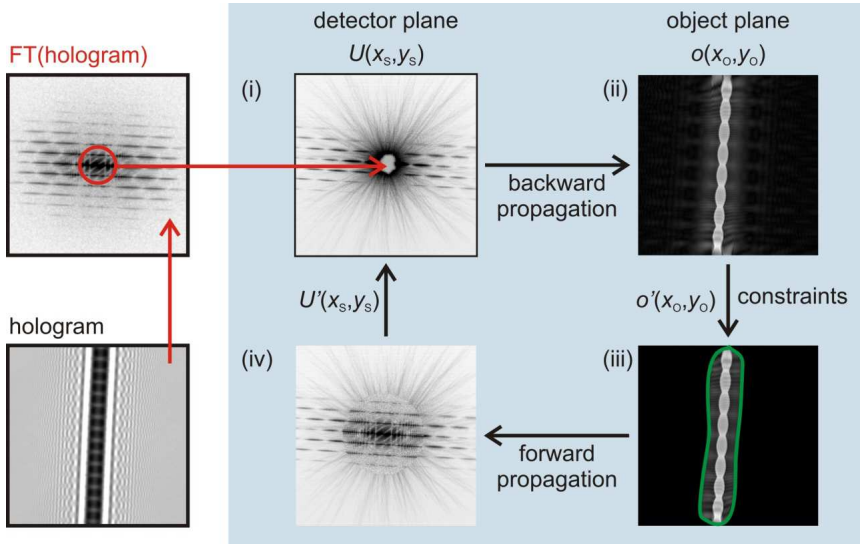

FIG. 16.3 –
Illustration describing the iterative reconstruction of a diffraction pattern of an object consisting of two twisted tungsten wires. The iterative loop includes the steps (i)-(iv) as described in the main text.

phase distribution of the object wave in the far-field detector plane. The diffraction pattern is then required to refine the reconstruction of the high-resolution information by a conventional iterative procedure. In addition, the central region of the diffraction pattern, which is usually missing, can be adapted from the amplitude of the Fourier transform of the hologram; see Fig. 16.3. The iterative procedure [4] includes the following steps as also illustrated in the flow-chart diagram in Fig. 16.3:

(i) Formation of the input complex-valued field in the detector plane $U(x_s, y_s)$. After each iteration, the amplitude of the field is given by the square root of the intensity of the diffraction pattern. The amplitude of the central part is provided by the amplitude of the Fourier transform of the hologram. The phase distribution is initially set to the phase of the Fourier transform of the hologram and it is updated after each iteration.

(ii) Back propagation to the object domain by inverse Fourier transform.

(iii) Two constraints are applied to the reconstructed complex-valued object distribution $o(x_o, y_o)$ resulting in a corrected function $o'(x_o, y_o)$. Since the object exhibits a finite size $o(x_o, y_o)$ is multiplied with a loose mask which sets the values outside a certain region to zero, see Fig. 16.3. Since the wave amplitude may not increase in the scattering process [5] the pixel values where absorption would become negative are also set to zero.

(iv) The forward propagation is calculated by the forward Fourier transform of $o'(x_o, y_o)$ and thus the complex-valued wavefront $U'(x_s, y_s)$ in the detector plane is obtained. Its amplitude and phase distributions are the input values for the next iteration starting at step (i).

This novel method for fast and unambiguous phase retrieval has recently been applied to experimental data of freestanding graphene as discussed next.

16.2.2 Graphene unit cell imaging by HCDI

We have shown that coherent diffraction with low-energy electrons allows imaging a freestanding graphene sheet of 210 nm in diameter with 2Å resolution. Ultra-clean graphene was prepared following our patented platinum metal catalysis method [7, 8]. A freestanding graphene sheet is placed over a 210 nm hole ion-milled into a platinum coated SiN membrane of 50 nm thickness. The entire sheet is reconstructed from just a single diffraction pattern displaying the arrangement of more than half a million individual graphene unit cells at once. The sheet is placed over a hole in a silicon nitride membrane and the impinging coherent parallel electron wavefront is formed by a micro-machined electron lens placed in front of the electron point source (see upper left part of Fig. 16.4 which essentially equals Fig. 16.1). The initial phase for the iterative phase refinement (see above) is provided by an in-line hologram of the same sample (Fig. 16.4 bottom left).

What remains to be done is to develop methods for depositing individual clusters onto such graphene sheets and decrease the electron wavelength to about 0.5Å to resolve the atomic structure of a nanometer-sized cluster.

Fig. 16.4 also shows a graphene hologram together with a coherent diffraction pattern of the very same region. In both experimental schemes, the source of the coherent electron beam consists of a sharp W(111) tip mounted on a 3-axis piezo-manipulator for positioning with nanometer precision. For the hologram the tip is brought as close as 380 nm to the sample. For the CDI recording the distance between the electron source and the micro-lens is approximately 8 microns and the distance between lens and sample amounts to approximately 200 microns. The diffraction pattern is recorded

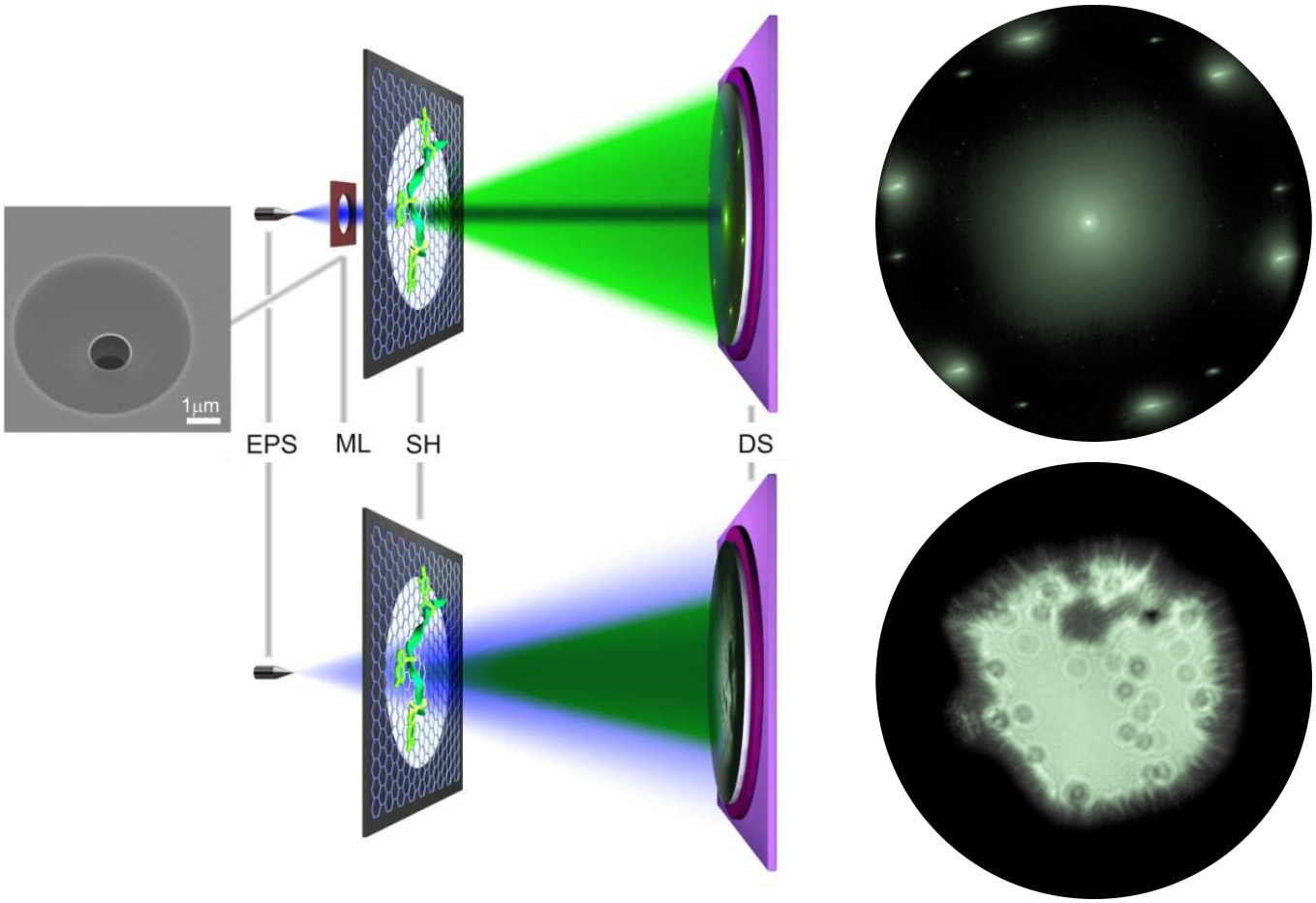

FIG. 16.4 –
Left: experimental arrangements for CDI (top) and holographic imaging (bottom) of freestanding graphene mounted on sample holder SH. See Fig.16.1 as well. The micro-lens (ML) in the CDI setup has a bore of 1 micron (see inset showing a SEM image of the lens). The detector system (DS) consists of a 75 mm diameter micro-channel-plate, followed by a phosphorous coated fibre-optic plate and a 8000×6000 pixels CCD chip.
Right: Images of freestanding graphene of 210 nm diameter resulting from the setups on the left. The diffraction pattern was taken with 236 eV electrons, the hologram with electrons of 58 eV. The outermost spots in the diffraction pattern correspond to 2.13Å as determined by the de Broglie wavelength of the electrons and the impact angle on the detector.

at 68 mm distance with a 8000×6000 pixels CCD chip with 75 mm diameter. The high dynamic range diffraction pattern is built up by combining three diffraction patterns taken with different exposure times. This pattern is then symmetrised by setting the intensity of each pair of centro-symmetric pixels to their average. Next, the diffraction pattern is transformed to spherical coordinates and multiplied with an apodization function to smoothen the edges. The number of pixels per unit cell is enhanced by zero-padding the diffraction pattern to 10,000×10,000 pixels. Accordingly, the hologram reconstruction was resampled to 10,000×10,000 pixels as well.

The overexposed region in the centre of the diffraction pattern is replaced by the corresponding 100 pixels in radius region of the square amplitude of the Fourier transform of the hologram [3]. The reconstruction uses the iterative procedure described in subsection 16.2.1. After 100 iterations, the entire 210 nm diameter freestanding graphene region is recovered with 2Å resolution, sufficient to display roughly 660'000 graphene unit cells (Fig. 16.5 left). Since there is no way to display the entire 10,000×10,000 image here, we have selected six square areas of 5 nm side length. The graphene unit cell is clearly apparent along with defects and domain boundaries present in the graphene sheet as anticipated for CVD grown graphene (Fig. 16.5 right).

To summarise, we have shown that low-energy electrons allow damage-free imaging of a 210 nm diameter graphene sheet with 2Å resolution. A single diffraction pattern, if sampled at a sufficiently high rate, provides a real-space image of more than half a million unit cells at once. Next, this graphene sheet will be used to support nanometer-sized clusters and images will be made with atomic resolution using ∼1 keV electrons.

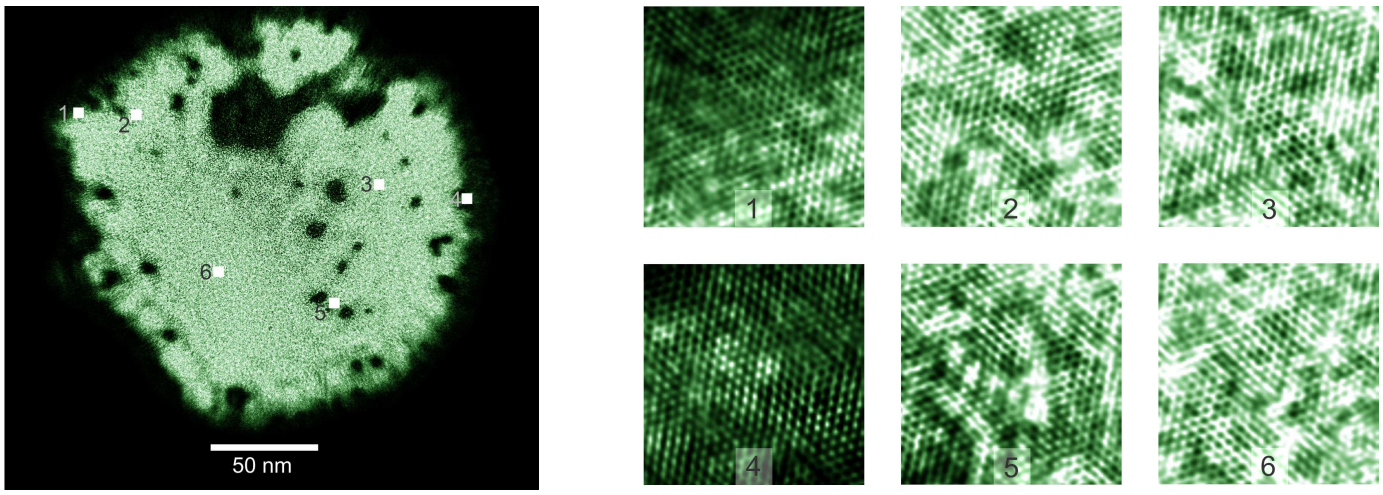

FIG. 16.5 – Left: Reconstruction of a 210 nm diameter freestanding graphene sheet. Expanded views of the six labelled 5×5 nm^2 areas are shown on the right.

16.3 Other recent achievements

- The HIM available at the EMPA enabled us to mill structures with 7 nm feature sizes, a prerequisite for FTH (see introduction) with electrons.
- The successful development of a procedure for a self aligned electron column made up of a micro-lens followed by an Einzel-lens.

16.4 Published results and theses

- A protein attached to a carbon nanotube could be imaged and cross-validated against TEM investigations in which the iron core of the protein (ferritin) could be imaged with high-energy electrons [6].
- A new method to achieve ultraclean freestanding graphene has been patented [7] and published [8].
- Clusters deposited on graphene were imaged by low-energy electron holography [9].
- A relationship between holography and coherent diffraction was found and exploited in an algorithm for fast and unambiguous phase retrieval [3].
- A method to improve the resolution in digital holography by self-extrapolation has been invented [10].
- Pulsed holography has been realised featuring a time resolution in the μs regime [11].
- The unit-cells of freestanding graphene have been imaged by coherent diffraction microscopy [12].
- Bachelor theses
  Jessica Britschgi: *4D Particle Tracking by Optical Holography revealed by manual tracking of microspheres in water from their holographic reconstructions*
  Beat Lauber: *Novel Fourier Transform Holography Setups*
- Master theses
  Simon Schwegler: *Sub-Pixel Registration Methods for Enhancement of Coherent Diffraction Images*
  Niklaus Waldvogel: *Assembly and Characterization of Tungsten Carbide Field Emitters*
  Simon Obrecht: *Thermal Desorption of Water from Green Fluorescent Protein (GFP)*
  Simon Bachmann: *Fabrication and Characterisation of ultra-clean Graphene by platinum metal catalysis* (in progress)

[1] M. Germann *et al.*, Phys. Rev. Lett. 104, 095501 (2010).
[2] E. Steinwand, J.-N. Longchamp, and H.-W. Fink, Ultramicroscopy 110, 1148 (2010).
[3] T. Latychevskaia, J.-N. Longchamp, and H.-W. Fink, Opt. Express 20, 28871 (2012).
[4] J. R. Fienup, Appl. Optics 21, 2758 (1982).
[5] T. Latychevskaia, and H.-W. Fink, Phys. Rev. Lett. 98, 233901 (2007).
[6] J.-N. Longchamp *et al.*, Appl. Phys. Lett. 101, 093701 (2012).
[7] J.-N. Longchamp, C. Escher, and H.-W. Fink, Patent, EP12189601.3 (2012).
[8] J.-N. Longchamp, C. Escher, and H.-W. Fink, J. Vac. Sci. Technol. B 31, 020605 (2013).
[9] J.-N. Longchamp *et al.*, Appl. Phys. Lett. 101, 113117 (2012).
[10] T. Latychevskaia, and H.-W. Fink, Opt. Express 21, 7726 (2013).
[11] M. Germann *et al.*, Appl. Phys. Lett. 102, 203115 (2013).
[12] J.-N. Longchamp *et al.*, Phys. Rev. Lett., Under review (2013).